ENHANCED APPROACH FOR BROACHING PREDICTION WITH HIGHER ORDER TERMS TAKEN INTO ACCOUNT

Hirotada HASHIMOTO[*1], **Naoya UMEDA**[*1] and **Akihiko MATSUDA**[*2]

[*1] Osaka University, Yamadaoka, Suita, 565-0871, Japan

h_hashi@naoe.eng.osaka-u.ac.jp , umeda@naoe.eng.osaka-u.ac.jp

[*2] National Research Institute of Fisheries Engineering, Hasaki, Kashima, 314-0421, Japan

amatsuda@fra.affrc.go.jp

SUMMARY

Based on a 4 degrees of freedom mathematical model proposed by the authors[1], its enhancement is attempted by taking most of the second order terms of waves into account for capsizing associated with surf-riding in following and quartering seas. This includes the wave effects on manoeuvring coefficients, the wave effects on restoring arm and so on. To confirm the prediction accuracy of each term the captive model experiments were systematically conducted. As a result, it is found that the wave effects on restoring moment are much smaller than the Froude-Krylov prediction and the minimum restoring arm appears on a wave downslope but not on a wave crest. Thus, an experimental formula of additional roll moment as hydrodynamic lift due to heel angle is provided for numerical modelling. Then numerical simulations are carried out with these second order terms of waves and compared with the results of free running model experiments. As a result, improvement of prediction accuracy for the ship motions in following and quartering seas are demonstrated. Although boundaries of ship motion modes are also calculated with both the original model and the present one, the second order terms of waves are not so crucial for prediction of the capsizing boundaries themselves. Moreover, we find that the wave-induced surge force and sway-roll coupling have certain nonlinearities with wave and sway velocity, respectively. As a result, the calculated capsizing boundary with these nonlinearities is reasonably improved.

NOMENCLATURE

a_H	interaction factor between hull and rudder
A_R	rudder area
c	wave celerity
d	mean draft
f_α	rudder lifting slope coefficient
F_n	nominal Froude number
g	gravitational acceleration
GZ	righting arm
GZ^{FK}	wave effect on righting arm with Froude-Krylov assumption
GZ^{WL}	wave effect on righting arm induced by hydrodynamic lift
H	wave height
I_{xx}	moment of inertia in roll
I_{zz}	moment of inertia in yaw
J	advance coefficient of propeller
J_{xx}	added moment of inertia in roll
J_{zz}	added moment of inertia in yaw
k	wave number
K_{NL}	nonlinear manoeuvring coefficients in roll
K_p	derivative of roll moment with respect to roll rate
K_r	derivative of roll moment with respect to yaw rate
K_r^W	wave effect on the derivative of roll moment with respect to yaw rate
K_R	rudder gain
K_T	thrust coefficient of propeller
K_v	derivative of roll moment with respect to sway velocity
K_v^W	wave effect on the derivative of roll moment with respect to sway velocity
K_w	wave-induced roll moment
K_δ	derivative of roll moment with respect to rudder angle
K_δ^W	wave effect on the derivative of roll moment with respect to rudder angle
K_ϕ	derivative of roll moment with respect to roll angle
l_R	correction factor for flow-straightening effect due to yaw rate
L	ship length between perpendiculars
m	ship mass
m_x	added mass in surge
m_y	added mass in sway
m_y^{2D}	2-dimensional added mass in sway
n	propeller revolution number
N_{NL}	nonlinear manoeuvring coefficients in yaw
N_r	derivative of yaw moment with respect to yaw rate
N_r^W	wave effect on the linear derivative of yaw moment with respect to yaw rate
N_v	derivative of yaw moment with respect to sway velocity
N_v^W	wave effect on the linear derivative of yaw moment with respect to sway velocity
N_w	wave-induced yaw moment
N_w'	$N_w' = N_w/(\rho L^2 d u^2/2)$
N_δ	derivative of yaw moment with respect to rudder Angle
N_δ^W	wave effect on the derivative of yaw moment with respect to rudder angle
N_ϕ	derivative of yaw moment with respect to roll

	angle
OG	vertical distance of centre of ship mass to water surface
p	roll rate
r	yaw rate
R	ship resistance
t	time
T	propeller thrust
T_D	time constant for differential control
T_E	time constant for steering gear
u	surge velocity
v	sway velocity
W	ship weight
w_p	effective propeller wake fraction
x_H	longitudinal position of centre of interaction force between hull and rudder
X_{NL}	nonlinear manoeuvring coefficients in surge
x_R	longitudinal position of rudder
X_w	wave-induced surge force
X_w'	$X_w' = X_w/(\rho L d u^2/2)$
X_{rud}	rudder-induced surge force
Y_{NL}	nonlinear manoeuvring coefficients in sway
Y_r	derivative of sway force with respect to yaw rate
Y_r^W	wave effect on the derivative of sway force with respect to yaw rate
Y_v	derivative of sway force with respect to sway velocity
Y_v^W	wave effect on the derivative of sway force with respect to sway velocity
Y_w	wave-induced sway force
Y_w'	$Y_w' = Y_w/(\rho L d u^2/2)$
Y_δ	derivative of sway force with respect to rudder angle
Y_δ^W	wave effect on the derivative of sway force with respect to rudder angle
Y_ϕ	derivative of sway force with respect to roll angle
z_H	vertical position of centre of sway force due to lateral motions
β	drift angle
χ	heading angle from wave direction
χ_c	desired heading angle for auto pilot
δ	rudder angle
ε_R	wake ratio between propeller and hull
ϕ	roll angle
γ_R	flow-straightening effect coefficient
κ_p	interaction factor between propeller and rudder
λ	wave length
ρ	water density
ξ_G	longitudinal position of centre of gravity from a wave trough
ξ_a	wave amplitude

1. INTRODUCTION

A practical ship complying with the current intact stability criteria of the International Maritime Organization (IMO) rarely capsizes in beam seas even in model scale but could occasionally capsize when she runs in following and quartering seas[2]. Although the IMO circulated just a simple guidance for avoiding danger in following and quartering seas applicable to all ships, real capsizing boundaries might depend on detailed particulars of each ship. Therefore, it is important to provide an operational guideline for each ship by utilising the most advanced theoretical prediction method.

International Towing Tank Conference (ITTC) recently established its specialist committee for benchmark testing of several numerical models for intact and damage stability[3]. For intact ships, according to comparisons between the numerical simulations and the results of free running model experiments, the mathematical model by Umeda et al. can qualitatively well predict broaching and surf-riding[1]. However, more improvement is necessary for a quantitative prediction. In this model, wave steepness and ship motions due to waves are assumed to be small. Thus second order terms of waves are consistently ignored as higher order terms for capsizing prediction.

Several mathematical models considering a part of them for improving prediction accuracy had been proposed so far, they were similar to or rather worse than the original model. The authors reported that, by adding the wave effects on manoeuvring forces, no significant improvement in time series were obtained[4]. In this paper, an enhanced mathematical model keeping the consistency as much as practical is developed by taking most of the second order terms of waves into account with help of systematic captive model experiments. Then the comparisons between the numerical results both with these terms and without them, as well as the results of the free running model experiments, are conducted to examine this new numerical prediction method as a more reliable prediction tool.

2. OUTLINE OF MATHEMATICAL MODELLING

The mathematical model of the surge-sway-yaw-roll motion was developed by Umeda and Renilson[5], Umeda and Vassalos[6] and Umeda[7] for capsizing associated with surf-riding in following and quartering waves, and we call the last one Original Model throughout this paper. The details of this model can be found in the literature[7]. Since wave steepness is much smaller than one, in the original model, drift angle, non-dimensional yaw rate, roll angle and rudder angle due to waves can be assumed to be as small as the wave steepness. Thus square terms and interaction terms of these elements are consistently ignored as higher order terms for capsizing prediction.

However, these higher order terms can be candidates for improving prediction accuracy towards more quantitative prediction, the authors upgrade the above-mentioned original model by taking most of the second order terms of waves into account. Two co-ordinate systems used here are shown in Figure 1: (1) a wave fixed with its origin at a wave trough, the ξ axis in the direction of wave travel; and (2) an upright body fixed with its origin at the centre of ship gravity. The state vector, $\mathbf{x}$ and control vector, $\mathbf{b}$, of this system are defined as follows:

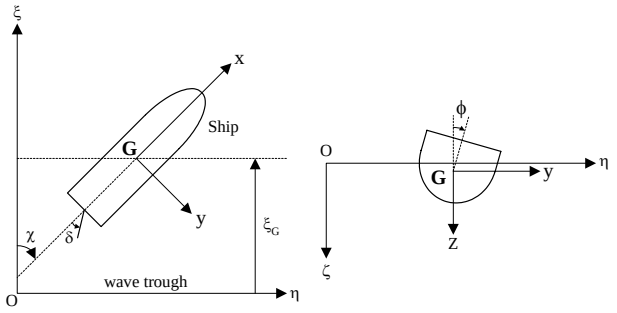

Figure 1: Co-ordinate systems

$$\mathbf{x} = (x_1, x_2, \cdots, x_8)^T = \{\xi_G / \lambda, u, v, \chi, r, \phi, p, \delta\}^T \quad (1)$$

$$\mathbf{b} = \{n, \chi_c\}^T \quad (2).$$

The upgraded dynamical system can be represented by the following state equation:

$$\dot{\mathbf{x}} = \mathbf{F}(\mathbf{x};\mathbf{b}) = \{f_1(\mathbf{x};\mathbf{b}), f_2(\mathbf{x};\mathbf{b}), \cdots, f_8(\mathbf{x};\mathbf{b})\}^T \quad (3)$$

where

$$f_1(\mathbf{x};\mathbf{b}) = (u\cos\chi - v\sin\chi - c)/\lambda \quad (4)$$

$$f_2(\mathbf{x};\mathbf{b}) = \{T(u;n) - R(u) + \underline{X_{NL}(u,v,r;n)} + \underline{X_{rud}(\xi_G/\lambda, u, \chi, \delta; n)} + X_w(\xi_G/\lambda, \chi)\}/(m + m_x) \quad (5)$$

$$f_3(\mathbf{x};\mathbf{b}) = \{-(m+m_x)ur + Y_v(u;n)v + \underline{Y_v^W(\xi_G/\lambda, u, \chi; n)v} + Y_r(u;n)r + \underline{Y_r^W(\xi_G/\lambda, u, \chi; n)r} + \underline{Y_{NL}(u,v,r;n)} + Y_\phi(u)\phi + Y_\delta(u;n)\delta + \underline{Y_\delta^W(\xi_G/\lambda, u, \chi; n)\delta} + Y_w(\xi_G/\lambda, u, \chi; n)\}/(m + m_y) \quad (6)$$

$$f_4(\mathbf{x};\mathbf{b}) = r \quad (7)$$

$$f_5(\mathbf{x};\mathbf{b}) = \{N_v(u;n)v + \underline{N_v^W(\xi_G/\lambda, u, \chi)v} + N_r(u;n)r + \underline{N_r^W(\xi_G/\lambda, u, \chi)r} + \underline{N_{NL}(u,v,r;n)} + N_\phi(u)\phi + N_\delta(u;n)\delta + \underline{N_\delta^W(\xi_G/\lambda, u, \chi; n)\delta} + N_w(\xi_G/\lambda, u, \chi; n)\}/(I_{ZZ} + J_{ZZ}) \quad (8)$$

$$f_6(\mathbf{x};\mathbf{b}) = p \quad (9)$$

$$f_7(\mathbf{x};\mathbf{b}) = [m_x z_H ur + K_v(u;n)v + \underline{K_v^W(\xi_G/\lambda, u, \chi; n)v} + K_r(u;n)r + \underline{K_r^W(\xi_G/\lambda, u, \chi; n)r} + \underline{K_{NL}(u,v,r;n)} + K_P(u)p + K_\phi(u)\phi + K_\delta(u;n)\delta + \underline{K_\delta^W(\xi_G/\lambda, u, \chi; n)\delta} + K_w(\xi_G/\lambda, u, \chi; n) + mg\{GZ(\phi) + \underline{GZ^{FK}(\xi_G/\lambda, u, \chi, \phi)} + \underline{GZ^{WL}(\xi_G/\lambda, u, \chi, \phi)}\}]/(I_{xx} + J_{xx}) \quad (10)$$

$$f_8(\mathbf{x};\mathbf{b}) = \{-\delta - K_R(\chi - \chi_C) - K_R T_D r\}/T_E \quad (11).$$

Here the underlined parts are newly added to the original model and nonlinear manoeuvring forces and moments in still water are expressed as follows:

$$X_{NL} = X_{vr}(u)vr + X_{vv}(u)v^2 + X_{rr}(u)r^2 + (m + m_y)vr \quad (12)$$

$$Y_{NL} = Y_{vvv}(u)v^3 + Y_{rrr}(u)r^3 + Y_{vvr}(u)v^2 r + Y_{vrr}(u)vr^2 \quad (13)$$

$$N_{NL} = N_{vvv}(u)v^3 + N_{rrr}(u)r^3 + N_{vvr}(u)v^2 r + N_{vrr}(u)vr^2 \quad (14)$$

$$K_{NL} = K_{vvv}(u)v^3 + K_{rrr}(u)r^3 + K_{vvr}(u)v^2 r + K_{vrr}(u)vr^2 \quad (15).$$

The wave forces are obtained as follows:

$$X_w(\xi_G/\lambda, \chi) = -\rho g \zeta_a k \cos\chi \int_{AE}^{FE} C_1(x) S(x) e^{-kd(x)/2} \sin k(\xi_G + x\cos\chi) dx \quad (16)$$

$$Y_w(\xi_G/\lambda, u, \chi; n) = \rho g \zeta_a k \sin\chi \int_{AE}^{FE} C_1(x) S(x) e^{-kd(x)/2} \sin k(\xi_G + x\cos\chi) dx + \zeta_a \omega\omega_e \sin\chi \int_{AE}^{FE} \rho S_y(x) e^{-kd(x)/2} \sin k(\xi_G + x\cos\chi) dx - \zeta_a \omega u \sin\chi [\rho S_y(x) e^{-kd(x)/2} \cos k(\xi_G + x\cos\chi)]_{AE}^{FE} + (1 + a_H)\frac{\rho}{2} A_R f_\alpha \varepsilon_R (1 - w_p) u \sqrt{1 + \kappa_P \frac{8K_T}{\pi J^2}} v_{WR} \quad (17).$$

Similarly, N_W and K_W can be obtained[8].

The wave effects on Y_v and Y_r as follows:

$$\begin{aligned} Y_v^W(\xi_G/\lambda, u, \chi; n) = {} & u\left[\zeta_r(x, \xi_G, \chi)\frac{\partial}{\partial z} m_y^{2D}(x,0)\right]_{AE}^{FE} \\ & - \left[u_w(x, \xi_G, \chi) m_y^{2D}(x,0)\right]_{AE}^{FE} \\ & + \int_{AE}^{FE} \frac{\partial u_w(x, \xi_G, \chi)}{\partial x} m_y^{2D}(x,0) dx \\ & + \frac{3}{2}(1 + a_H)\rho A_R f_\alpha \gamma_R u_w(x, \xi_G, \chi) \end{aligned} \quad (18)$$

$$\begin{aligned} Y_r^W(\xi_G/\lambda, u, \chi; n) = {} & u\left[x\zeta_r(x, \xi_G, \chi)\frac{\partial}{\partial z} m_y^{2D}(x,0)\right]_{AE}^{FE} \\ & - \left[u_w(x, \xi_G, \chi) x m_y^{2D}(x,0)\right]_{AE}^{FE} \\ & - 2\int_{AE}^{FE} u_w(x, \xi_G, \chi) m_y^{2D}(x,0) \\ & + \int_{AE}^{FE} \frac{\partial u_w(x, \xi_G, \chi)}{\partial x} x m_y^{2D}(x,0) dx \\ & + \frac{3}{2}(1 + a_H)\rho A_R f_\alpha \gamma_R l_R u_w(x, \xi_G, \chi) \end{aligned} \quad (19).$$

Similarly, N_v^W, N_r^W, K_v^W and K_r^W can be obtained[4].

Furthermore, the wave effects on Y_δ can be estimated by applying the concept of MMG model, expressed as follows:

$$Y_\delta^W(\xi_G/\lambda, u, \chi; n) = (1 + a_H)\frac{\rho}{2} A_R f_\alpha \{2\varepsilon_R(1 - w_p)u \times \sqrt{1 + \kappa_p \frac{8K_T}{\pi J^2}} u_w(x, \xi_G, \chi)\} \quad (20).$$

Similarly, N_δ^W and K_δ^W can be obtained[9].

3. CAPTIVE MODEL EXPERIMENTS

To confirm prediction accuracy of the above-mentioned modelling, captive model experiments of a 135 gross tonnage purse seiner used as the subject ship of the ITTC benchmark testing were conducted at a

seakeeping and manoeuvring basin of National Research Institute of Fisheries Engineering. Body plan and principal particulars of the subject ship are shown in Figure 2 and Table 1, respectively. The 1/17.25 scaled model of the ship fitted with a turning table was towed by an X-Y towing carriage in long-crested regular waves. The model was equipped with a rudder but without a propeller. By adjusting the towing velocities of two directions, the drift angle and the heading one were independently realised. The longitudinal force, the lateral force, the turning moment, the heel moment and the rudder normal force were measured by dynamometers. Here the model was free in heave and pitch and fixed in surge, sway, yaw and roll.

The experiments cover various forward velocities, drift angles, heel angles, rudder deflections and heading angles. In addition, model runs were repeated with the wave steepness of 1/25, 1/20, 1/15 as well as in calm water. Manoeuvring coefficients can be identified by following standard procedures for the case both in calm water and in waves. Then, wave effects can be obtained as difference between the measured results in waves and those in calm water. Comparison results between the theories and the experiments in the wave effects on manoeuvring coefficients will be published in a separate paper[9].

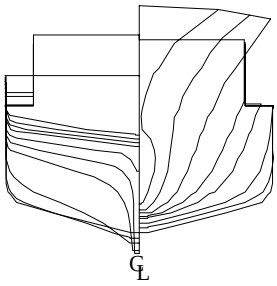

Figure 2: Body plan of the subject ship

Table 1: Principal particulars of the subject ship

Items	*Values*
length : L_{pp}	34.5 m
breadth : B	7.60 m
depth : D	3.07 m
mean draught : d	2.65 m
block coefficient : C_b	0.597
longitudinal position of centre of gravity from the midship : x_{CG}	1.31 m aft
metacentric height : GM	1.00 m
natural roll period : T_ϕ	7.4 s
rudder area : A_R	3.49 m^2
time constant of steering gear : T_E	0.63 s
proportional gain: K_P	1.0
time constant for differential control: T_D	0.0 s
maximum rudder angle: δ_{max}	$\pm 35^\circ$

4. WAVE EFFECTS ON RESTORING ARM

It is widely accepted that restoring arm decreases when the ship centre situates on a crest of longitudinal waves[10]. It is also believed that this phenomenon can be explained by integrating wave pressure up to wave surface with the Froude-Krylov assumption[10-11]. However, in the benchmark testing programme of the ITTC committee, whenever we included the wave effect on restoring arm, prediction of extreme motions became rather worse[3]. Thus we use the captive test results with the subject ship model for identifying the restoring moment acting on the hull. Here the model was towed with the heel angle of 10 degrees in waves. By excluding components due to forward motion with the heel angle in calm water and wave exciting moment acting on the upright hull, the measured wave effect on restoring arm was identified, and then is compared with the calculation based on the Froude-Krylov assumption. Here the incident wave pressure is integrated up to the incident wave surface and the Smith effect is also taken into account[11].

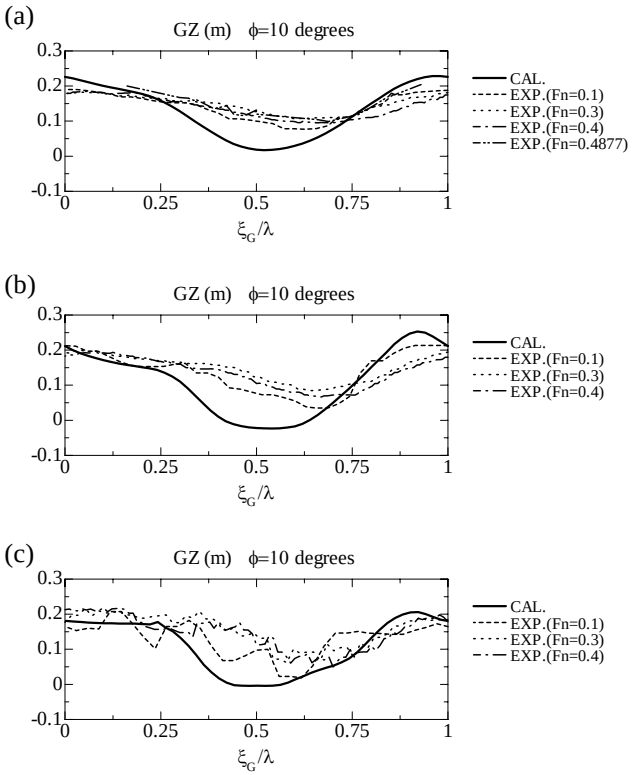

Figure 3: Comparisons of righting arm between the calculation based on Froud-Krylov assumption and the experiment for the ship with (a) H/λ=1/25, λ/L=1.5, χ=0 degrees, (b) H/λ=1/15, λ/L=1.5, χ=0 degrees and (c) H/λ=1/15, λ/L=1.5, χ=30 degrees

The comparisons between the measured and calculated values are shown in Figure 3. The measured amplitudes are smaller than the calculated ones and the minima of the restoring arm exist at wave downslope near wave crests. This observation is applicable for various wave steepness, Froude numbers and heading angles. This means that the

Froude-Krylov assumption cannot completely explain the wave effect on restoring arm. Here the Froude number of 0.4877 in the heading angle of 0 degrees corresponds to exactly zero encounter frequency of the model to waves.

The difference between the measured values and the Froude-Krylov component can be explained as follows. Since a centre of sectional under-water area moves in horizontal direction when a ship rolls, she has a hull-form-camber line, which is equivalent to camber line of the wing section. Therefore a lift force acts on a submerged hull with forward velocity in horizontal direction[12-13]. As a result, roll moment that reduces a righting moment is induced. Its schematic view is provided in Figure 4. The aft-end section is dominant for lift force according to a slender body theory[14]. When a centre of gravity of a ship is situated on a wave crest, the lift force is smaller because draught and added mass in lateral direction are smaller at the aft-end section. Thus, on a wave crest, this component in the restoring moment is larger than that in calm water. By contrast, when a centre of gravity of a ship is situated on a wave trough, the lift force is larger. Thus, on a wave trough, this component in the restoring moment is smaller. In addition, the attack angle of the hull-form-camber is smaller on a wave crest while the attack angle is larger on a wave trough at least for this wave length to ship length ratio. Therefore, the hydrodynamic lift due to the hull-form-camber reduces the wave effect on restoring arm. Here, however, the lift coefficient cannot be regarded as constant and can be done rather as a function of the Froude number because free surface effect on the coefficient is significant[13].

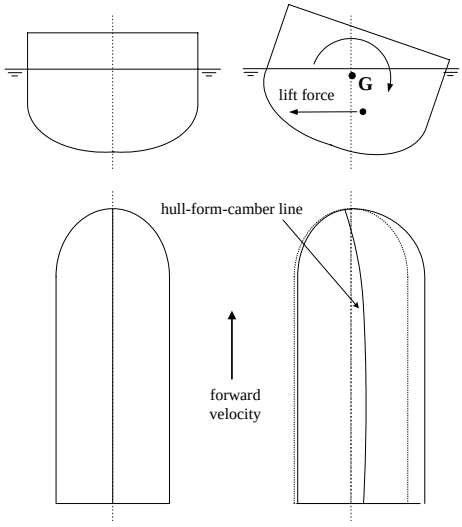

Figure 4: Schematic view of a hull-form-camber line and induced lift force and moment

Based on the above thought and fitting to the measured results, the hydrodynamic component of the wave effect on restoring arm is modelled as follows:

$$GZ^{WL} = [\{(7.4\times e^{-7.9\times Fn})(-\zeta_a \cos(2\pi\xi_G/\lambda + 0.314)) + (18.6\times e^{-9.2\times Fn})\times(2\zeta_a)^2/L\}\times\phi\times\frac{1}{2}\rho L d u^2\}]\times H_{eff}\times(\frac{d}{2}-OG)/W \quad (21)$$

where

$$H_{eff} = \sqrt{\frac{2\pi\frac{L}{\lambda}\cos(\chi)\sin\left(\pi\frac{L}{\lambda}\cos(\chi)\right)}{\pi^2-\left(\pi\frac{L}{\lambda}\cos(\chi)\right)^2}} \quad (22).$$

Here the lift coefficient is assumed to change as the function of the wave elevation, the Froude number and heel angle. In addition, to consider wavelength to ship length ratio and heading angle, Grim's effective wave concept is used[15]. In this formulation third order terms of waves are also taken into account for explaining the average value of the restoring arm because this value is not so small to be ignored. The wave effects on restoring moment can be obtained by adding the outcomes of above formula to the Froude-Krylov components. It is noteworthy that this formula can be applied only for the subject ship and applicability to other ships should be investigated in future.

5. COMPARISONS BETWEEN NUMERICAL SIMULATIONS AND MODEL EXPERIMENTS

The comparisons of numerical simulations between the enhanced mathematical model and the original one as well as the free running model experiments[2] are carried out. For the numerical simulations, the initial values of state variables are estimated with the same procedure used for the ITTC benchmark testing[3].

Firstly, the comparison for the case that the ship experiences a periodic motion is shown in Figure 5. The absolute yaw angle calculated with the original model is much smaller than the measured one while with the enhanced model it is closer to the measured one. This is because the constant force is induced by the product of periodically varying manoeuvring coefficients and periodic lateral motions. This also improves prediction accuracy of other motions.

Secondly, the comparison for the case of a ship suffering surf-riding and broaching is shown in Figure 6. The calculation with the original model provides shorter capsizing time than the experiment while with the enhanced model it shows longer capsizing time. In the calculation with the original model, the yaw angular velocity has been significant until capsizing. However, in that with the enhanced model, the ship seems to be on an unstable equilibrium at the time of 10 seconds and then capsizes with help of the reduction of transverse stability. The experimental results are similar to the latter model. Obviously the introduction of the wave effects on restoring arm realises this improvement.

The comparison of boundaries of ship motion modes with the original model and present one is shown in Figure 7. The procedure and the judging criteria used in this calculation can be found in the literature[16]. Here the each nominal Froude number of the experiment is not a specified value but the measured one in average because the propeller revolution was not completely constant

during the experiment. In higher speed zone, the region of *stable surf-riding* obtained with the enhanced model is wider than that with the original one and the region of *capsizing due to broaching* is narrower. However, the boundaries between *periodic motion* and *capsizing* do not depend on the difference of the numerical model very much. Therefore, the higher order terms that discussed in this paper are not so very important for prediction of the capsizing boundaries themselves.

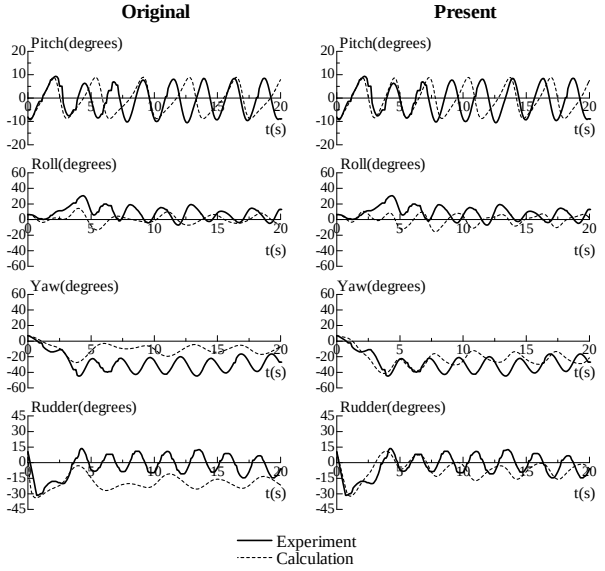

Figure 5: Comparison between the numerical results with the enhanced mathematical model and those with original one and experimental results with H/λ=1/10, λ/L=1.637, χ=-30 degrees and F_n=0.3

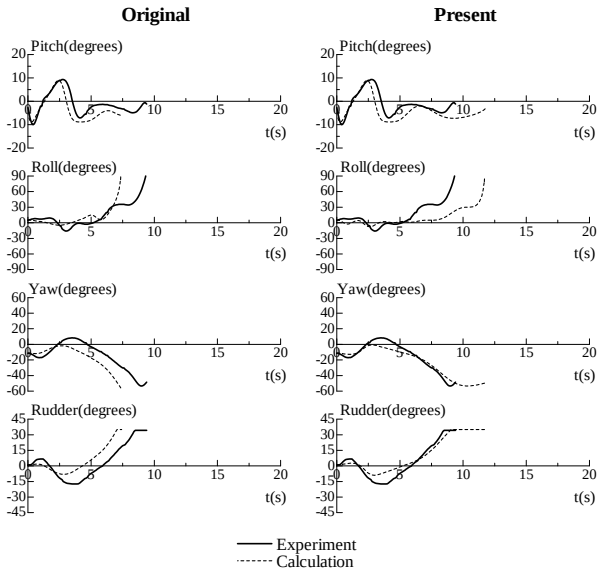

Figure 6: Comparison between the numerical results with the enhanced mathematical model and those with original one and experimental results with H/λ=1/10, λ/L=1.637, χ=-10 degrees and F_n=0.43

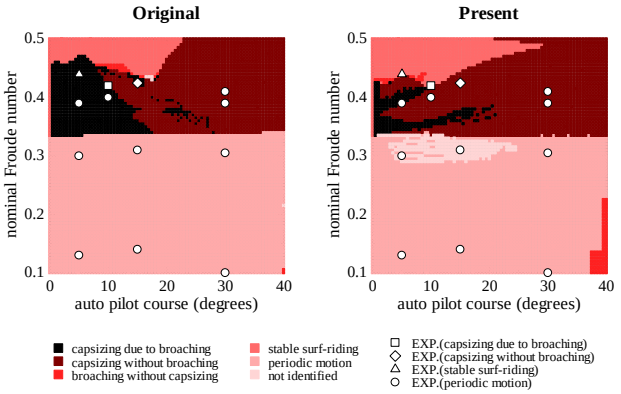

Figure 7: Comparison between numerical results with the enhanced mathematical model, those with original mathematical model and the experimental results with H/λ=1/10, λ /L=1.637 and the initial periodic state for F_n =0.1, χ_C=0 degrees

6. EFFECTS OF NONLINEAR WAVE FORCES AND NONLINEAR SWAY-ROLL COUPLING

Responding to these outcomes, we revisit prediction accuracy of wave forces, especially wave-induced surge force, because the calculated capsizing boundaries at zero heading angles correspond to the surf-riding threshold. Therefore, the comparisons of wave forces between experiment and theoretical prediction are carried out and those results are shown in Figures 8-9. As a result, agreement between the experiment and the calculation is fairly good as reported for a trawler before[8] but some nonlinearily of the wave-induced surge force amplitude can be found. Then we obtained a correction curve by fitting to the ratio in amplitude between the measured value and linearly calculated one as shown in Figure 10. These nonlinear relationships between the surge force and the wave may consist of several hydrodynamic components discussed in Umeda[17]. By contrast, there is no significant nonlinearity in the wave-induced sway force and the wave-induced yaw moment as shown in Figures 11-12. These also indicate that constant components due to the second order wave contributions are negligibly small.

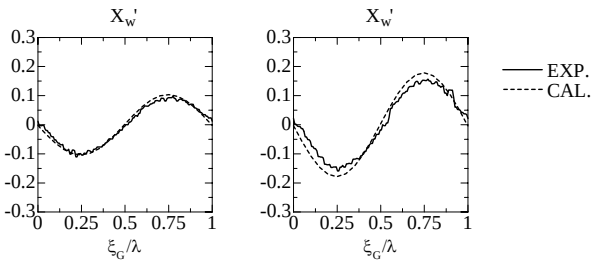

Figure 8: Comparisons of wave-induced surge force between the experiment and the linear theory (left: H/λ=1/25, λ/L=1.5, χ=0degrees, right: H/λ=1/15, λ/L=1.5, χ=0 degrees)

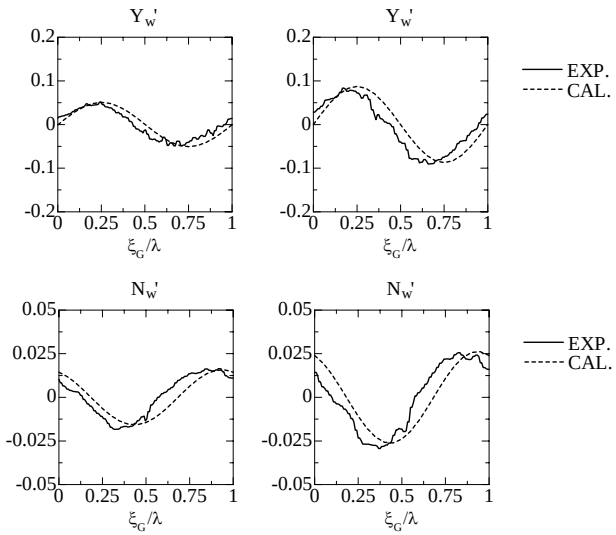

Figure 9: Comparisons of wave-induced sway force and yaw moment between the experiment and the linear theory (left: H/λ=1/25, λ/L=1.5, χ =15 degrees, right: H/λ=1/15, λ/L=1.5, χ =15 degrees)

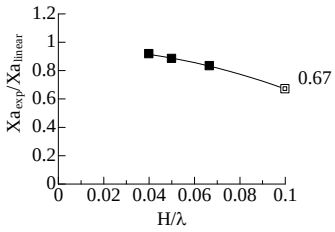

Figure 10: The ratio of the measured wave-induced surge force amplitude to that of the linear theory where χ=0 degrees

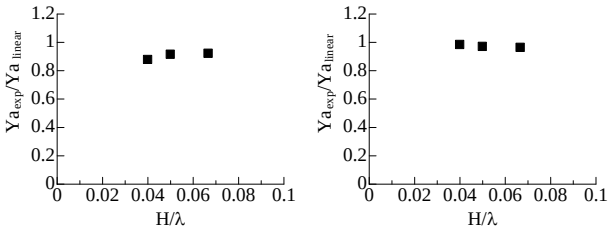

Figure 11: The ratio of the measured wave-induced sway force amplitude to that of the linear theory (left: χ=15 degrees, right: χ=30degrees)

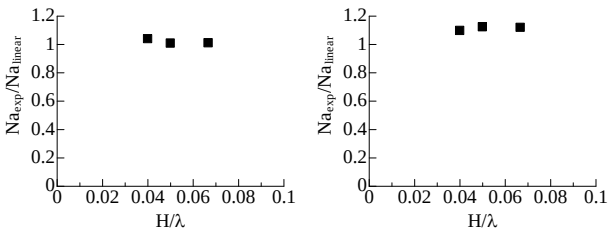

Figure 12: The ratio of the measured wave-induced yaw moment amplitude to that of the linear theory (left: χ=15 degrees, right: χ=30degrees)

By considering the above-mentioned nonlinearity of the wave-induced surge force, the boundaries of ship motion modes are calculated. As a result, the calculated critical Froude number of capsizing becomes considerably larger and closer to the experimental one. However, it decreases in the range over 30 degrees of auto pilot course and this result does not correspond to experimental results even in qualitatively.

By comparing contributions from all terms, we examine the dominant factors that lead to be such an outcome. As a result, we find that the nonlinearity of the vertical position of centre of sway force due to lateral motions with respect to drift angle, z_H, e.g. sway-roll coupling effect, is not too small to be ignored while it is assumed to be linear so far. Then the correction curve is obtained by fitting to the experimental data in calm water as shown in Figure 13. Finally, the boundaries of ship motion modes with nonlinearity of the wave-induced surge force and that of z_H taken into account are calculated, as shown in Figure 14. The newly obtained lower limit of capsizing is much closer to the measured results both in the original and the present model than the previous ones shown in Figure 7. These results indicate that the nonlinearity of sway-roll coupling could prevent an excessive heel due to large sway velocity at larger auto pilot course and is also important for more reasonable prediction.

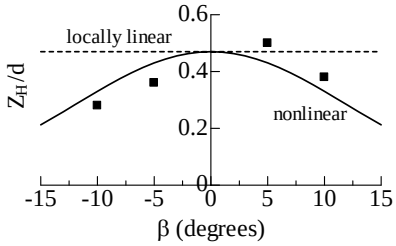

Figure 13: The measured vertical position of centre of sway force due to lateral motions with respect to drift angle (symbols) with linear and nonlinear fitted curves

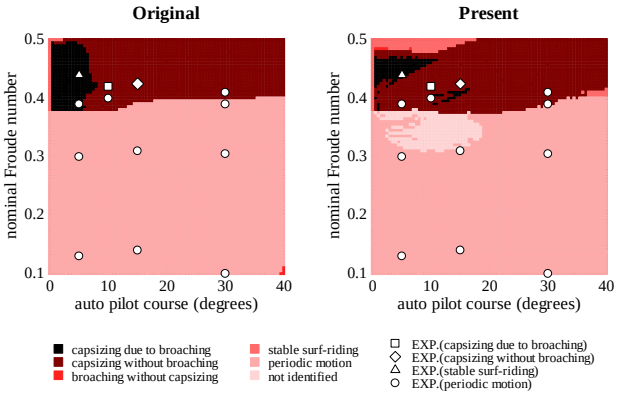

Figure 14: Comparison between numerical results with the nonlinear wave-induced surge force and the sway-roll coupling and the experimental results with H/λ=1/10, λ /L=1.637 and the initial periodic state for F_n =0.1, χ_C=0 degrees

7. CONCLUSIONS

A mathematical model taking most of the second order terms with respect of waves into account is proposed with a series of captive experiments, and is compared with existing free running experiments. As a result, the following conclusions are provided:

1. The wave effects on restoring moment cannot be always accurately estimated with the Froude-Krylov assumption, but can be supplemented with experimental results of varying hydrodynamic lift due to heel angle.
2. By taking the second order terms of waves into account, prediction accuracy of the numerical simulation in time domain for ship motions in following and quartering seas is improved.
3. The second order terms of waves are not so important to predict the capsizing boundaries themselves.
4. Prediction accuracy of wave forces is generally good but nonlinearlity of the wave-induced surge force is found.
5. Nonlinearity of the wave-induced surge force, as well as the nonlinear sway-roll coupling, improves accuracy of prediction on capsizing boundary to some extent.

8. ACKNOWLEDGMENTS

The authors would like to express his sincere gratitude to Dr. M.R. Renilson, Qinetiq, for his useful discussion. This research was supported by a Grant-in Aid for Scientific Research of the Ministry of Education, Culture, Sports, Science and Technology of Japan (No. 13555270).

9. REFERENCES

1. Umeda N, Munif A, Hashimoto H (2000) Numerical prediction of extreme motions and capsizing for intact ships in following/quartering seas, In: *Proceedings of the 4th Osaka colloquium on seakeeping performance of ships*, Osaka, 368-373
2. Umeda N, Matsuda A, Hamamoto M and Suzuki S (1999) Stability Assessment for Intact Ships in the Light of Model Experiments, *J Mar Sci Technol*, 4:45-57
3. Umeda, N. and M.R. Renilson, (2001) Benchmark Testing of Numerical Prediction on Capsizing of Intact Stability in Following and Quartering Seas, In: *Proceedings of the 5th International Stability Workshop*, Trieste, pp 6.1.1-10
4. Hashimoto H. and Umeda, N. (2001), "Importance of Wave effects on Manoeuvring Coefficients for Capsizing Prediction", In: *Proceedings of the 5th International Stability Workshop*, 6.4.1-8
5. Umead N, Renilson MR (1992) Broaching -a dynamic behaviour of a vessel in following seas-. In: *Wilson PA (ed) Manoeuvring and control of marine craft*. Computational Mechanics Publications, Southampton, pp 533-543
6. Umeda N, Vassalos D (1996) Non-linear periodic motions of a ship running in following and quartering seas. *J Soc Nav Archit Jpn* 179: 89-101
7. Umeda N (1999) Nonlinear dynamics of ship capsizing due to broaching in following and quartering seas. *J Mar Sci Technol* 4: 16-26
8. Umeda N, Yamakoshi Y and Suzuki S (1995) Experimental Study for Wave Forces on a Ship Running in Quartering Seas with very Low Encounter Frequency, In: *Proceedings of the Sevastianov Symposium*, Kaliningrad
9. Umeda N, Hashimoto H and Matsuda A (2002) Broaching Prediction in the Light of an Enhanced Mathematical Model with Higher Order Terms Taken into Account, (to be appeared)
10. Paulling J.R. (1961) The Transverse Stability of a Ship in a Longitudinal Seaway, *J Ship Research*, 4: 37-49
11. Hamamoto M and Nomoto K (1982) Transverse Stability of Ships in a Following Sea, In: *Proceedings of the 2nd International Conference on Stability of Ships and Ocean Vehicles*, Tokyo, 215-224
12. Eda H (1980) Rolling and Steering Performance of High Speed Ships -Simulation Studies of Yaw-Roll-Rudder Coupled Instability-, In: *Proceedings of the 13th Symposium of Naval Hydrodynamics*, *J Soc Nav Archit Jpn*, 427-439
13. Obrastsov W.B. (1966) Experimental Investigation of Influence of Ship's Speed on its Transverse Stability, In: *Proceedings of Leningrad Shipbuilding Institute*, 89-97 (in Russian)
14. Lighthill, M.J. (1960), Note on the Swimming of Slender Fish, *J Fluid Mech*, 9: 305-317
15. Grim O (1961) Beitrag zu dem Problem der Sicherheit des Schiffes im Seegang, *Shiff und Hafen*, 6: 490-497 (in German)
16. Umeda N, Hashimoto H (2002) Qualitative Aspects of Nonlinear Ship Motions in Following and Quartering Seas with High Forward Velocity, *J Mar Sci Technol*, 6: 111-121
17. Umeda N (1984) Resistance Variation and Surf-riding of a Fishing Boat in Following Sea, *Bulletin of National Research Institute of Fisheries Engineering*, 5: 185-205